ELSEVIER

Marine Geology 175 (2001) 221–235

MARINE GEOLOGY
INTERNATIONAL JOURNAL OF MARINE GEOLOGY, GEOCHEMISTRY AND GEOPHYSICS

www.elsevier.nl/locate/margeo

Abrupt change in slope causes variation in the deposit thickness of concentrated particle-driven density currents

Thierry Mulder[a,*], Jan Alexander[b]

[a]*Department of Earth Sciences, Cardiff University of Wales, PO Box 914, Cardiff, CF1 3YE, UK*
[b]*School of Environmental Sciences, University of East Anglia, Norwich, NR4 7TJ, UK*

Received 8 October 1999; accepted 17 January 2001

Abstract

Abrupt changes in slope occur frequently in some marine environments. Laterally confined laboratory experiments show that when dense surge-like particulate flows travel over abrupt slope reductions their deposits may have an asymmetric bell-shaped thickening near the break of slope. This thickening is herein called a slope-break deposit and is related to the change in kinetic energy of the flow. Slope-break deposits are particularly pronounced under relatively high-velocity flows. In our experiments these are flows with high particle concentrations ($c = 5–10\%$ by volume silicon carbide) moving down slopes steeper than 3°. The experiments were designed such that currents generated by a lock-exchange mechanism flowed down a slope (variable slope angle) onto a flat surface. The bodies of the flows became thicker and slower just downstream of the slope break. Because the flow body slows very rapidly, particles are dumped forming the slope-break deposit. The peak in sediment thickness of the slope-break deposit is downstream of the break in slope because falling particles continue to move forward in the flow during settling. The slope-break deposits may be several tens of percent thicker than deposits from an equivalent flow in which no change in slope occurred. The parameters of the slope-break deposit correlate with slope angle change.

1. Introduction

Density currents are a frequent mechanism of sediment transport in offshore environments (Nardin et al., 1979). The general term 'density current' includes classical turbidity currents in which most of the current is dominated by particle support by fluid turbulence (Middleton and Hampton, 1973) and other density currents in which particle concentration is higher and all particles are not maintained in complete turbulent suspension (Mulder and Alexander, in press). Some density currents generate substantially thick and extensive deposits (Hughes-Clarke et al., 1990; Masson, 1994; Syvitski and Schafer, 1996). The deposits can form good hydrocarbon reservoirs, and therefore, prediction of local increase in deposit thickness would be useful for understanding reservoir geometry and targeting exploration drilling.

The seafloor is not a flat or uniformly sloping surface, but rather changes in slope are common at various scales. Seafloor morphology relates to the history of deposition, erosion and tectonic activity. Changes of slope can be gradual, as is generally the case at the base of continental slope (Adams and Schlager, 2000), or more abrupt, as for example, at the base of a tectonic ramp or the mouth of some submarine canyons or

* Corresponding author: Département de Géologie et Océanographie, CNRS UMR 5805 EPOC, Université Bordeaux 1, Avenue des Facultés, 33405 Talence cedex, France. Tel: + 330-556-848847; Fax: + 330-556-840848.

E-mail address: t.mulder@geocean.u-bordeaux.fr (T. Mulder).

0025-3227/01/$ - see front matter
PII: S0025-3227(01)00114-1

channels. At sites of abrupt slope reduction flow energy declines and changes in deposition rate and erosional potential affect the seafloor morphology. This paper considers flow behaviour and deposit character at sites of abrupt slope reduction. Natural submarine density currents can not easily be observed directly, but they can be visualised by observing either analogous flows (e.g. sedimentary or volcanic flows on land) or laboratory experiments. This paper considers the latter despite the amount of caution that is need when comparing results from laboratory experiments and natural processes (see for example discussions by Middleton, 1966a,b,c, 1967, 1993; Kneller and Buckee, 2000). A ramp-flat design was used for the laboratory experiments as a basis for comparison with flows in tectonically active basins, such as the modern Gulf of Corinth (Papatheodorou and Ferentinos, 1993; Collier et al., 2000) or the Early Jurassic North Sea Basin (Rooksby, 1991) and for comparison with other sites of abrupt submarine slope change, such as the Var channel mouth (discussed below). Submarine channel geometry often changes rapidly at sites of natural abrupt slope change and density currents may be free to spread laterally. In the experiments presented here, however, the currents were laterally confined (2-D) to isolate the influence of slope change from that of lateral spreading. The experiments use an angular change in slope as: (a) it is easier to construct and (b) the point of slope change is easily defined so that its exact position can be related to changes observed in the flow and deposits. In reality, sediment deposition near the base of slopes over time will tend to produce more gradual slope changes (except perhaps at the foot of active faults, or actively eroded scarps). Even with such sediment accumulation, however, the change in gradient is often over a short distance relative to the gravity current runout distance.

A rapid reduction in gradient can generate a drop in flow velocity combined with an increase in flow thickness (Komar, 1971) and has the potential to generate a hydraulic jump. Hydraulic jumps form when the hydraulic regime of a flow changes from supercritical (Froude number, $Fr > 1$) to subcritical ($Fr < 1$). The densiometric Froude number is defined as:

$$Fr = \frac{V}{\sqrt{g h_b \cos\alpha \dfrac{\rho_f - \rho_a}{\rho_a}}} \quad (1)$$

where g is the gravitational acceleration (9.81 ms^{-1}), ρ_f is the density of the flow, ρ_a is the ambient water density, h_b is the height of the body of the flow, α is the bed slope and V is the mean forward velocity. Menard (1964) recognised that hydraulic jumps could occur in turbidity currents, when flow experienced a rapid change of slope or width. The sedimentary implications of a change in flow geometry, potentially associated with a hydraulic jump, have been discussed for other settings such as water flow (Carling, 1995; Chanson and Montes, 1995), pyroclastic surges (Cole and Scarpati, 1993), marine shelves (Adams et al., 1990; Sarkar et al., 1991) and periglacial streams (Gorrell and Shaw, 1991), but in general the deposits are still poorly known. Komar (1971, 1975) estimated the critical slope for a density current to create a hydraulic jump in the range from 0.1 to 2% (0.05–1.15°), consistent with our experimental set-up. Weirich (1988, 1989) described abrupt thickening of a gravity-current deposit associated with a channel expansion and break in slope in an artificial lake that he attributed to a hydraulic jump. The deposit thickening occurred just downstream of the change in slope. Natural turbidites have also been observed to change character across abrupt changes in slope, for example Piper and Savoye (1993) described deposits of the 1979 Nice event just pass the Var Canyon mouth and an abrupt change in slope steepness. This example is considered in more detail below.

Bed shear stress and current velocity decrease across a hydraulic jump according to the continuity equation of water flux (Komar, 1973). Flow velocity can decrease by as much as a half through a hydraulic jump (Komar, 1971; Garcia and Parker, 1989). Flow thickness increases accordingly to the same continuity equation forming a definable feature in free-surface flows where the upper boundary can be observed directly. In subaqueous density currents, however, slope change can influence the amount of mixing between the flow and ambient fluid. Such mixing in our laboratory experiments obscured the upper flow surface making identification of the position of hydraulic jumps difficult.

Garcia and Parker (1989) used laboratory experiments to investigate the change in turbidity current flow regime through a hydraulic jump resulting from a decrease in bed slope. Their currents had low sediment concentration and could not be used to document deposit variations related to the hydraulic jump. Garcia

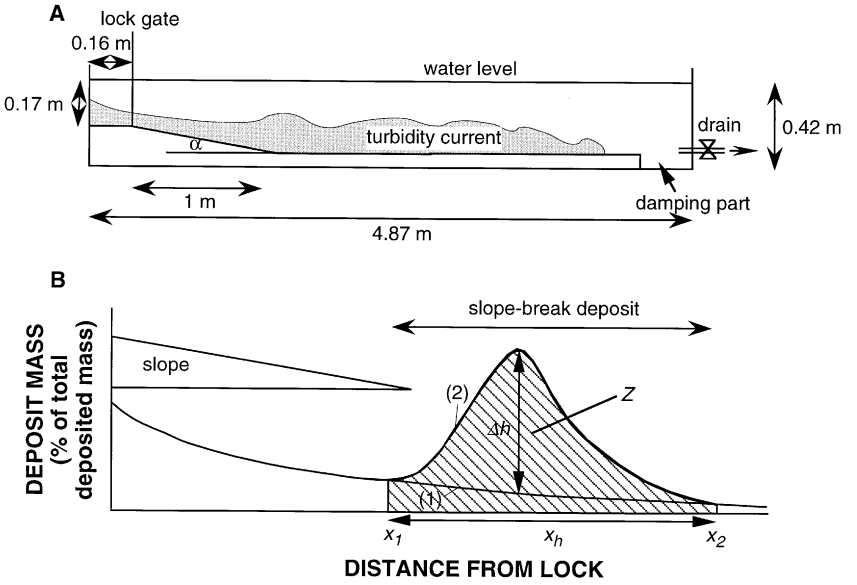

Fig. 1. (A) Experimental tank and (B) Notation and symbols used for the study of slope-break deposits. Note that (A) and (B) are drawn at different scales.

(1993), however, noted that the break in slope controlling the formation of the hydraulic jump seemed to cause a reduction in the rate at which the deposits thinned with distance. He showed that bedload deposition occurs quickly after the jump due to bed shear stress reduction. Owing to the velocity reduction and increase in flow-thickness across a hydraulic jump, there may be a loss of competence (grain size that can be transported) and capacity (amount of sediment that can be transported) through a hydraulic jump. Consequently, a reduced rate of bed thinning (Garcia, 1993) or an increase in bed thickness across, or just downstream of a hydraulic jump should be expected, with a concomitant change in deposit grain size or sorting.

This paper demonstrates that significant changes in turbidite thickness can be related to abrupt changes in slope that might or might not have created hydraulic jumps in the flow and that the extent and amplitude of the bed thickness increase depends on that change in slope.

2. Experimental conditions and apparatus

Concentrated density currents were generated in a long tank (4.87 m long, 0.17 m wide, 0.42 m deep) by the release of particle–water mixtures into fresh water using a lock-exchange mechanism (Fig. 1). The mixture was composed of moderately sorted (standard deviation = 0.72 μm) silicon carbide particles ($\rho_s = 3220$ kg m^{-3}) with a mean equivalent spherical diameter of 51 μm. Two initial solid volume concentrations (c_i) were used: $c_i = 5$ and 10%.

The particles were mixed vigorously with water in the lock until the moment that the lock gate was opened (Alexander and Morris, 1994). The resulting turbid surge (as defined by Ravenne and Beghin, 1983) flowed down a 1 m-long incline onto a horizontal surface (Fig. 1A). The incline angle (α) was varied and data are presented from runs with slopes of 0, 3, 6, 9 and 12°. Most of the surges did not reach the distal end of the tank and even the fastest and most prolonged surges (10% initial concentration on a 12° slope) had a velocity less than 0.05 ms^{-1} at the end of the tank. Consequently, the distal ends of the flows were only weakly affected by reflected flow from the tank end-wall. A damping area, with tank floor a little lower than the experimental flat reach (Fig. 1), minimised the impact of any reflected sediment-transporting flow. The depth of the experimental tank is only about two times the thickness of the flow, and therefore, return flow in the active upper

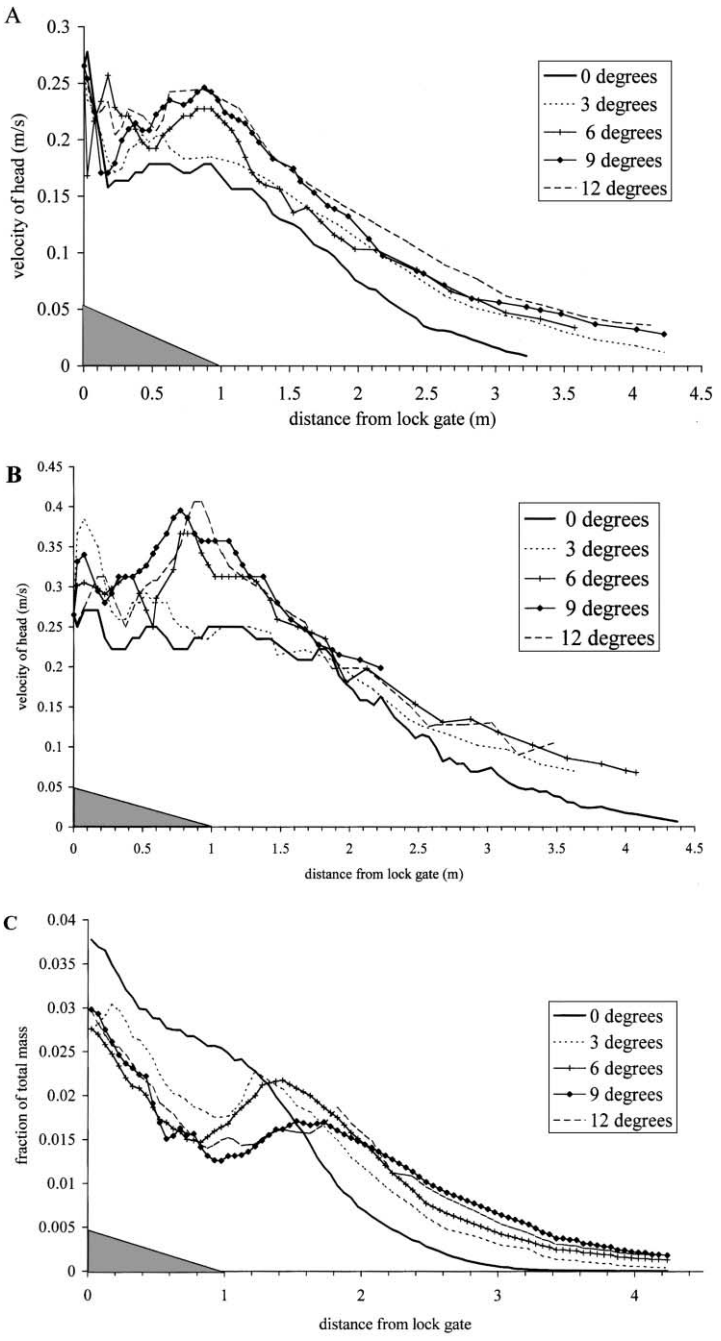

Fig. 2. Experimental results. Head velocity for $c_i = 5\%$ (A) and $c_i = 10\%$ (B). Mass distribution for the total deposits of runs with $c_i = 5\%$ (C) and $c_i = 10\%$ (D). The velocity curves are smoothed using a three point moving average (smoothing over a 15cm moving window).

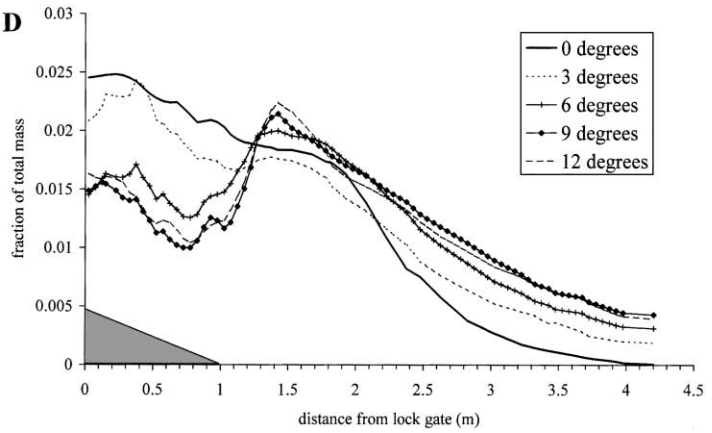

Fig. 2. (*continued*)

layer is more important in the experiments than in natural deep-water conditions (Huppert and Simpson, 1980). Head velocity and flow thickness were measured from high speed video records with a precision of 0.04 s. It was not possible to measure velocities within the body of the surges because of their opacity, the presence of a mixing cloud, and the short duration of the flow events. The distribution of deposit mass was measured by siphoning sediment from sample areas along the tank floor. The samples were filtered and dried before weighing. The grain size of ten samples, with sampling intervals increasing with distance from the lock gate, was analysed using a Sedigraph.

3. Experimental results

On opening the lock gate, the suspension collapsed into the tank to form a short duration and unsteady surge. Equivalent surges (same initial concentration and volume) released onto slopes attained and maintained greater head velocities and travelled further than those released on the flat tank floor (Fig. 2A and B). The velocity of the head approaching the base of slope was proportional to the slope angle. Beyond the break of slope the head velocity of all flows declined gradually, although just beyond the slope break the flows going through a greater slope change decelerated more. At most distal sites the head velocity of different flows of equivalent starting conditions varied with the slope angle in the proximal reach. At or near the break of slope the body of the flow just behind the head thickened and remained thick as the body passed. This thickening corresponded to growing billows and rapid mixing-cloud development. As the flows waned the area of flow thickening near the break in slope became indistinct in the tail of the flow. This behaviour is distinctly different from the development of hydraulic jumps in long-duration currents observed by Garcia and Parker (1989).

Comparison of deposits between runs with differing initial conditions is made by considering the mass distribution relative to the total mass of deposits outside the lock in that run (Fig. 2C and D). On this basis deposits were generally thinner on steeper slopes. Deposits of surges released onto slopes extended farther down the tank than deposits of equivalent surges on the flat tank floor (as observed also by Rimoldi et al., 1996) and the steeper the slope the further the deposits extended (Fig. 2C and D).

All surges released on slopes had an increase in deposit mass at or near the break of slope (Fig. 2C and D). This correlates with an increase in bed thickness in this area. Beyond the slope break, after an initial increase, deposit mass decreased with distance. Where the mass increased just past the slope break, the deposits had an asymmetrical bell-shape in cross-section parallel to flow (Fig. 2C and D), herein termed a ‘slope-break deposit’. The peak in

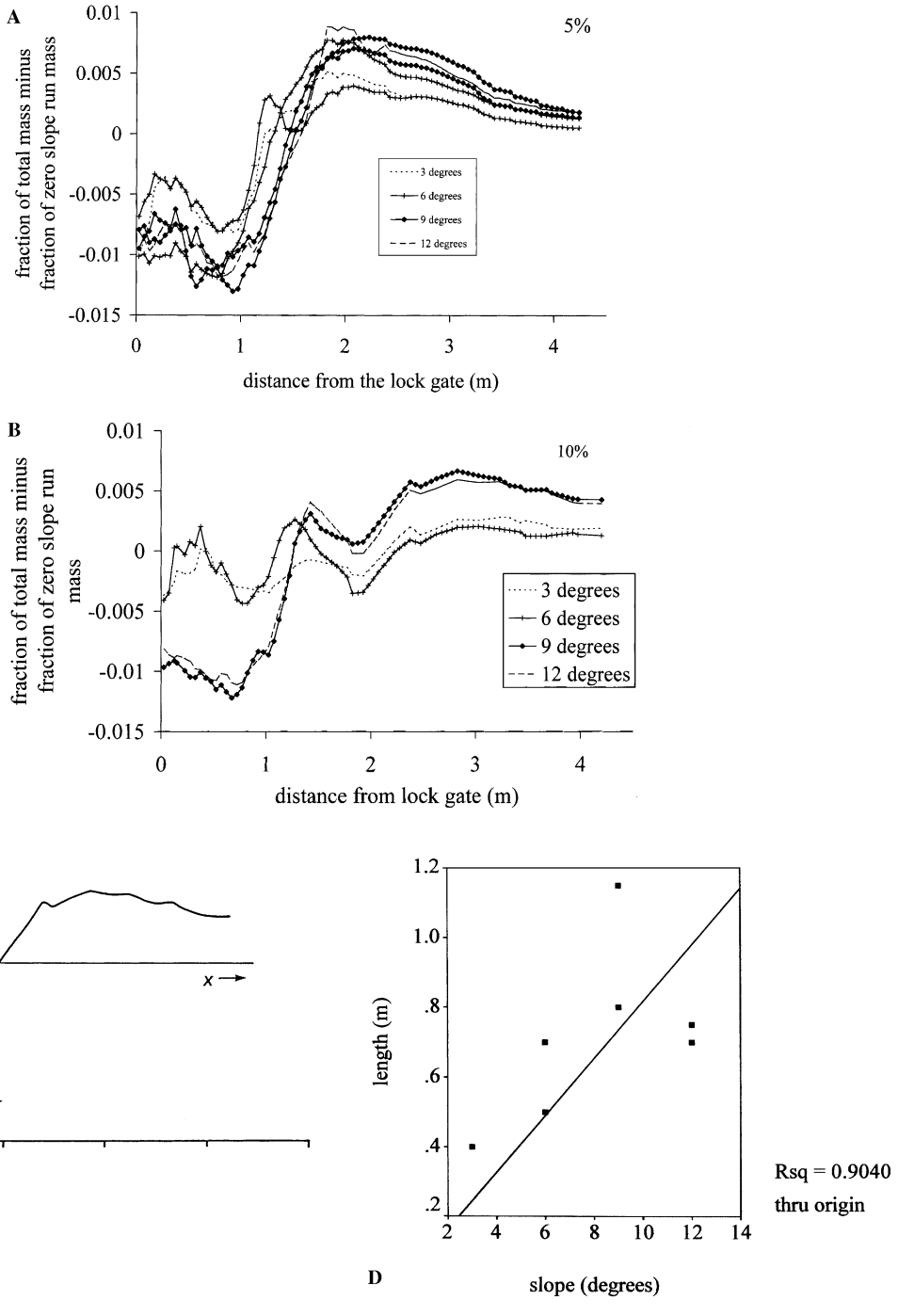
A
5%
fraction of total mass minus fraction of zero slope run mass
0.01
0.005
0
-0.005
-0.01
-0.015
3 degrees
6 degrees
9 degrees
12 degrees
0
1
2
3
4
distance from the lock gate (m)
B
10%
fraction of total mass minus fraction of zero slope run mass
0.01
0.005
0
-0.005
-0.01
-0.015
3 degrees
6 degrees
9 degrees
12 degrees
0
1
2
3
4
distance from lock gate (m)
x
A
xh
C
1.2
1.0
.8
.6
.4
.2
length (m)
2
4
6
8
10
12
14
slope (degrees)
D
Rsq = 0.9040
thru origin

Fig. 3.

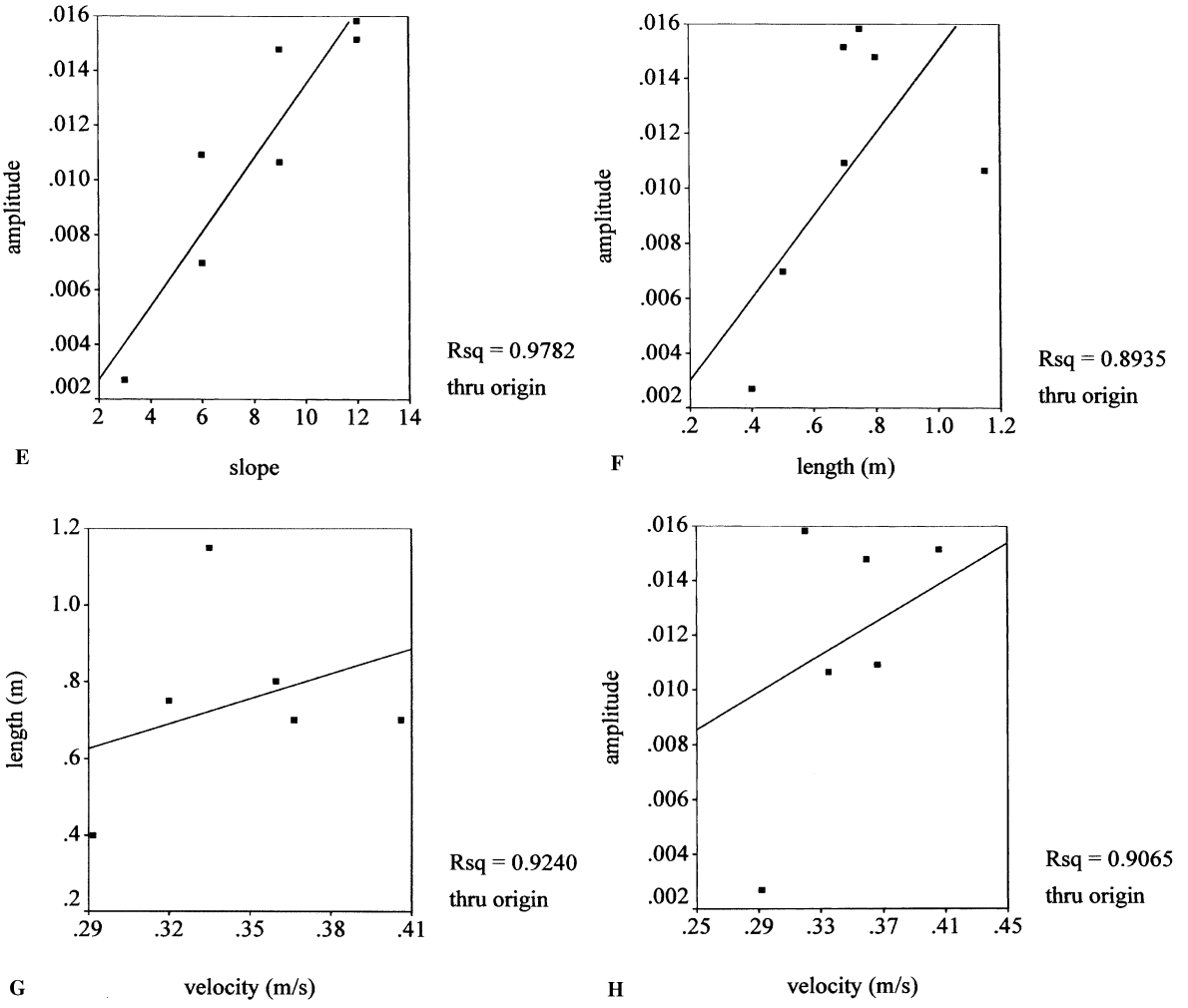

Fig. 3. Graphs to show relationships for slope-break deposits calculated using method 1. The mass distribution as a fraction of total mass relative to the mass distribution of an equivalent flow on a zero slope for runs (method 1) with: (A) initial solid concentration of 5%, (B) 10%, (C) Definition diagram for a break of slope deposit using this method of estimation. The *y*-axis is the mass of a sample as a fraction of the total mass of the deposit relative to the mass distribution of an equivalent flow on a zero slope. *y*-axis values can range from −1 to +1, (D) Length of slope-break deposit against slope angle calculated from method 1, (E) Amplitude of slope-break deposit against slope angle calculated from method 1, (F) Amplitude of slope-break deposit against length, (G) Slope-break deposit length against maximum velocity of the head of the flow on the slope and (H) Amplitude of slope-break deposit against maximum velocity of the head of the flow on the slope.

deposit mass that is related to the decrease in slope, occurs downflow of the point where the flow velocity drops and the flow thickness increases. This happens because the settling particles fall through a moving fluid and reach the bed at a distance downstream from the point where they began to fall within the surge. This distance depends on flow thickness, particle size and density. As noted by Garcia and Parker (1989), this dispersion of particles downstream of a hydraulic jump is more significant if particles have small fall velocity. We could not assess the variation in slope-break deposit dimensions with settling velocity, as the sediment used was uniform in grade and density.

4. Defining the dimensions of the slope-break deposit

Laval et al. (1988) suggested that in the absence of slope, deposit thickness decays exponentially with distance. However, Dade et al. (1994) found that on a uniform and gentle slope, deposit thickness decayed exponentially in the far field area down stream of a self-similar region. In this study the zero slope runs were similar to Dade et al.'s (1994) mass distribution pattern and the onset of the exponential decline in mass occurred at about 150 and 200 cm from the lock gate (for $c_i = 5$ and 10% respectively). Dade et al. (1994) predict that greater slope angle generates longer runout distances and decreased proximal bed thickness, 'stretching' the deposit. This change in deposit distribution is observed in the proximal 1 m of our experiments. The slope break imposes a change on the flow but the pattern of deposition does not simply change to that of the new (zero) slope. In other words the mass of the deposit does not simply decline at a faster rate from the break in slope, but rather there is an area of greater deposit thickness near the break of slope.

Two methods are used to define the slope-break deposit and to estimate the effect of an abrupt reduction in slope on deposit distribution in these experiments. Method (1) compares observed mass distribution with equivalent deposits on zero slope. This is calculated by subtracting the mass distribution data from that of an equivalent run on a 0° slope. Method (2) subtracts a simulated exponential curve (from the point corresponding to the beginning of slope) from the observed mass distribution. The disadvantage of the first method is that it can not isolate the effect of the proximal slope from that of the change of slope and so may exaggerate the influence of the break of slope. The second method may hide the influence of the change in flow behaviour inherent from the geometry of the lock and mechanism of flow generation (i.e. the mass pattern on a uniform slope is not a simple exponential curve cf. Dade et al., 1994). This problem is partly overcome by using the same method to consider the apparent local mass excess in the zero slope examples. Method (1) can not be applied to natural deposits as the nature of the original flow is generally unknown and so deposits of an equivalent flow on a zero slope can not be generated.

Using the 1st method the distributions of deposit mass relative to the equivalent mass distribution on zero slope are presented in Fig. 3A and B. These confirm that the deposits tend to be thinner in proximal areas and thicker in distal areas compared to equivalent zero slope runs. These plots suggest that the flows on low gradient slopes (3° and some 6°), that pass over a low angle change in bed-slope behave slightly differently to those on steeper slopes.

In all of the runs there is an abrupt change from negative to positive, relative to the equivalent zero slope run, just beyond the position of the break of slope. This change is particularly abrupt in runs with $c_i = 10\%$, but is also visible in runs with $c_i = 5\%$. After an initial increase in relative mass, there is a dip in the curves, confirming that the mass pattern is not a simple transition from that on an inclined surface to that on a zero slope, but rather that there is an area of enhanced mass near the break of slope: a slope-break deposit. It is difficult to define a slope-break deposit for most of the 5% runs using this method.

Using method 1, the proximal end of the slope-break deposit (x_1) is defined at the first minimum on the relative mass curves (in the 10% runs only), the distal end (x_2) at the second minimum, and the length of the slope-break deposit (x_h) is the distance between the two minima. The position of the distal end of the deposit defined in this way does not vary significantly between runs. The proximal end varies slightly with slope angle and as a consequence there is a relationship between change in slope and the deposit length defined by method 1 (Fig. 3D).

The amplitude of the deposit is defined as the difference between the first minimum and first maximum beyond the break of slope (Fig. 3C). There is a very good relationship between slope (and consequently slope angle change) and deposit amplitude (Fig. 3E), and as intuitively expected, a good relationship between deposit length and amplitude (Fig. 3F).

The maximum velocity of the head on the slope is defined as V_1, the velocity at the distal end of the slope-break deposit is V_2. The deceleration from the slope to the end of the slope-break deposit, $\mathrm{d}V/\mathrm{d}t$, is approximated by $V\mathrm{d}V/\mathrm{d}x$.

$$V\frac{\mathrm{d}V}{\mathrm{d}x} \approx \frac{(V_1 + V_2)}{2} \cdot \frac{(V_2 - V_1)}{(x_2 - x_1)} = \frac{(V_2^2 - V_1^2)}{2(x_2 - x_1)} \quad (2)$$

The relationship of both slope-break deposit length and amplitude with head velocity on the slope (V_1) and head deceleration is less well defined by the experimental data than is the relationship with slope angle change (Fig. 3G and H). The deposit amplitude must depend on the velocity change in the body of the flow (controlling capacity change) but also turbulence intensity and flow thickness. All of these may change at the slope-break. Unfortunately we were unable to measure velocity within the body of the flow.

The strongest relationship defined by the experimental data using method 1 is between the slope-break deposit amplitude and the change in slope (equivalent to proximal slope in these experiments). The length of a slope-break deposit represents the time/distance lag because of the finite time taken for sediment to settle to the bed through the thickness of the flow following the change in flow behaviour triggered by the slope break. The length must therefore be controlled by the flow thickness, settling velocity of particles and velocity within the flow. In contrast the amplitude of the slope-break deposit is controlled by the change in flux of sediment to the bed resulting from the change in flow behaviour. Because it is controlled by the change in flux, the flow thickness (and change in flow thickness caused by the slope change) may be less important. Consequently the amplitude may be more directly related to the magnitude of the change in slope. There is, as intuitively expected, a relationship between amplitude and deposit length, but the scatter on the deposit amplitude/length graph (Fig. 3F) reflects the difference in the degree of control on the two dimensions.

The second method of assessing the geometry of the area of mass excess of the slope-break deposit involves fitting an exponential curve to the experimental deposit-mass data (curve 1 on Fig. 1B). The upstream point where the experimental data depart from the exponential curve is located at or just upstream of the position of the slope break and this is defined as the upstream end of the slope-break deposit (x_1 on Fig. 1B). The projected exponential curve merges with the measured curve at x_2 that is defined as the distal end of the slope-break deposit (Fig. 1B). The distance between x_1 and x_2 represents the extent of the slope-break deposit (x_h). The amplitude of the slope-break deposit is the difference between the two curves at the point of maximum deposition. The total mass of sediment corresponding to the area of the slope-break deposit (between x_1 and x_2) expressed as a percentage of the total mass is Z.

There are strong relationships between α, x_h (Fig. 4a) and Z (Fig. 4b). The correlation of x_h with α may indicate that the departure from the exponential is longer with slope because it takes longer to reach the far-field conditions (Dade et al., 1994). The relationship x_h: α and Z: α are a little different for the runs with different initial concentration. The slope-break deposit length is generally less for lower initial concentration flows and the dispersion around the correlation lines in Fig. 4a may, in part, result from the variation in initial concentration due to small differences in the manual mixing before the lock gate was opened. In general these data suggest that the slope-break deposits have similar geometry but are generally smaller for the less dense flows. The strong relationship between x_h and Z (Fig. 4e) is intuitively obvious as given the same sediment concentration and grain size the longer the area of deposits sampled, the greater will be the mass of the sample.

Correlation between the parameters of the slope-break deposit and the maximum velocity of the head measured on slope (V_1 is the same in both methods) are presented in Fig. 4c and d. This velocity is controlled by the concentration and the slope and consequently reflects the real concentration (i.e. the hypothetical concentration modified by the degree of perfection of the initial manual mixing in the lock). There is overlap between the x_h and V_1 data from the two experimental sets and both sets have a very similar relationship trend. Moreover, the use of velocity allows us to provide unified equations for all the runs rather than separate relationships for each initial concentration. This confirms the suggestion above (using method 1) that the slope-break deposit length records the lag time for the particles to reach the bed following the change in flow conditions and this is controlled primarily by flow velocity and settling velocity. The sediment properties are the same in all of the runs so that differences in x_h relate directly to velocity and the length relationship appears to be independent of initial sediment concentration. Fig. 4c and d show x_h and Z correlate with V_1 suggesting

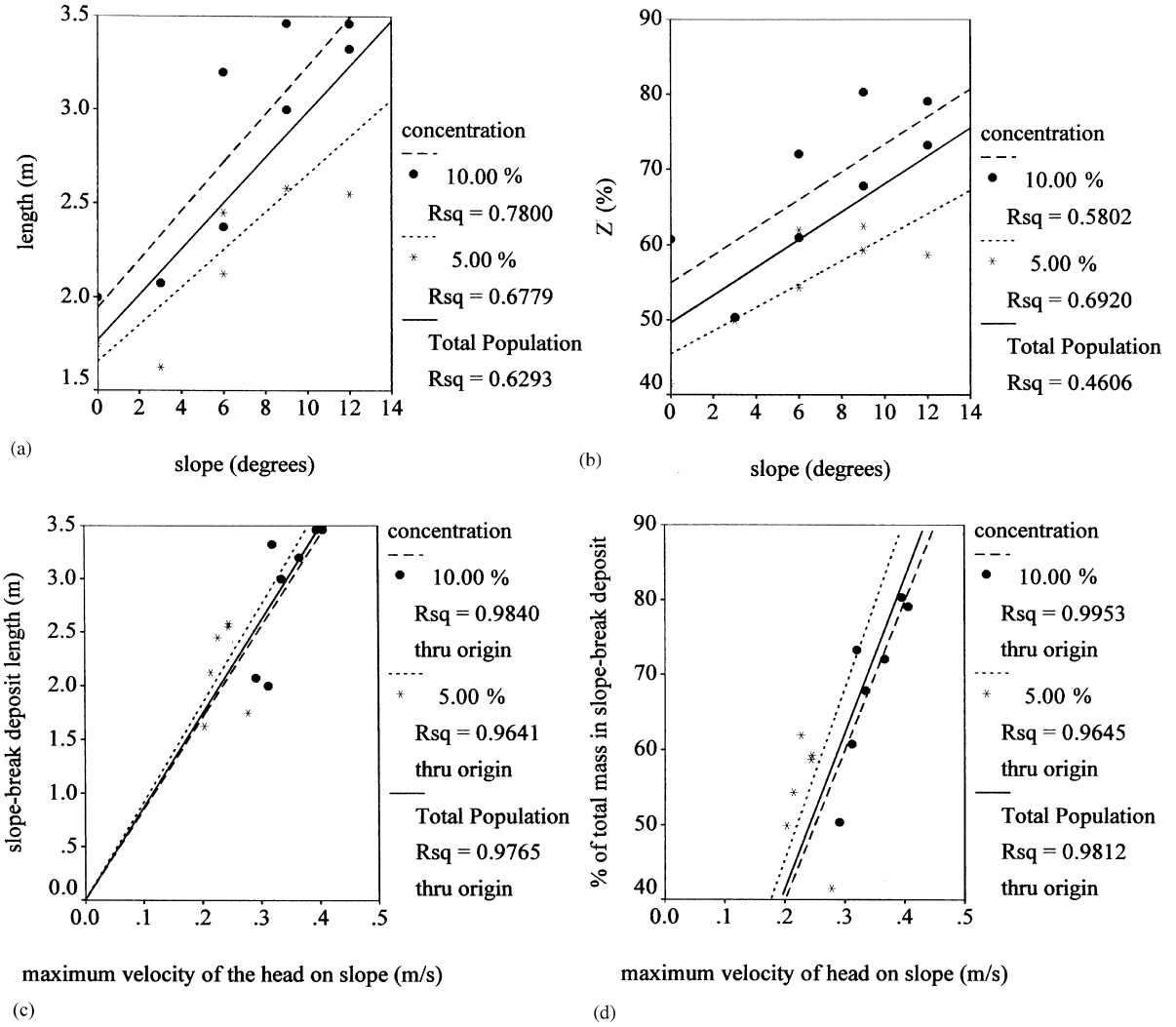

Fig. 4. Graphs to show relationships for slope-break deposits calculated using method 2. (a) Relationship between slope and the flow-parallel extent of the slope-break deposit, (b) slope angle and the total sediment mass of the slope-break deposit, (c) Flow-parallel extent of the slope-break deposit against the maximum head velocity on the slope, (d) Total sediment mass of the slope-break deposit expressed as a percentage of the total mass against the maximum head velocity on the slope, (e) The flow-parallel extent of the slope-break deposit against the total sediment mass of the slope-break deposit, (f) Total sediment mass of the slope-break deposit expressed as a percentage of total mass against flow deceleration and (g) Length of the slope-break deposit against flow deceleration.

deceleration just past the slope break is more important when initial velocity is high.

At the point (x_2 on Fig. 1B) where the projected exponential curve merges with the measured curve (curve 2 on Fig. 1B), the velocity of the head is V_2, this is defined differently from method 1 as the defined distal ends of the slope-break deposits are different. Plotting Z and x_h as functions of $(V_2^2 - V_1^2)/2(x_2 - x_1)$ (Fig. 4f and g) suggests that the relationship between slope-break deposit dimensions and deceleration of the head of the flow over the length of the deposit is not straightforward.

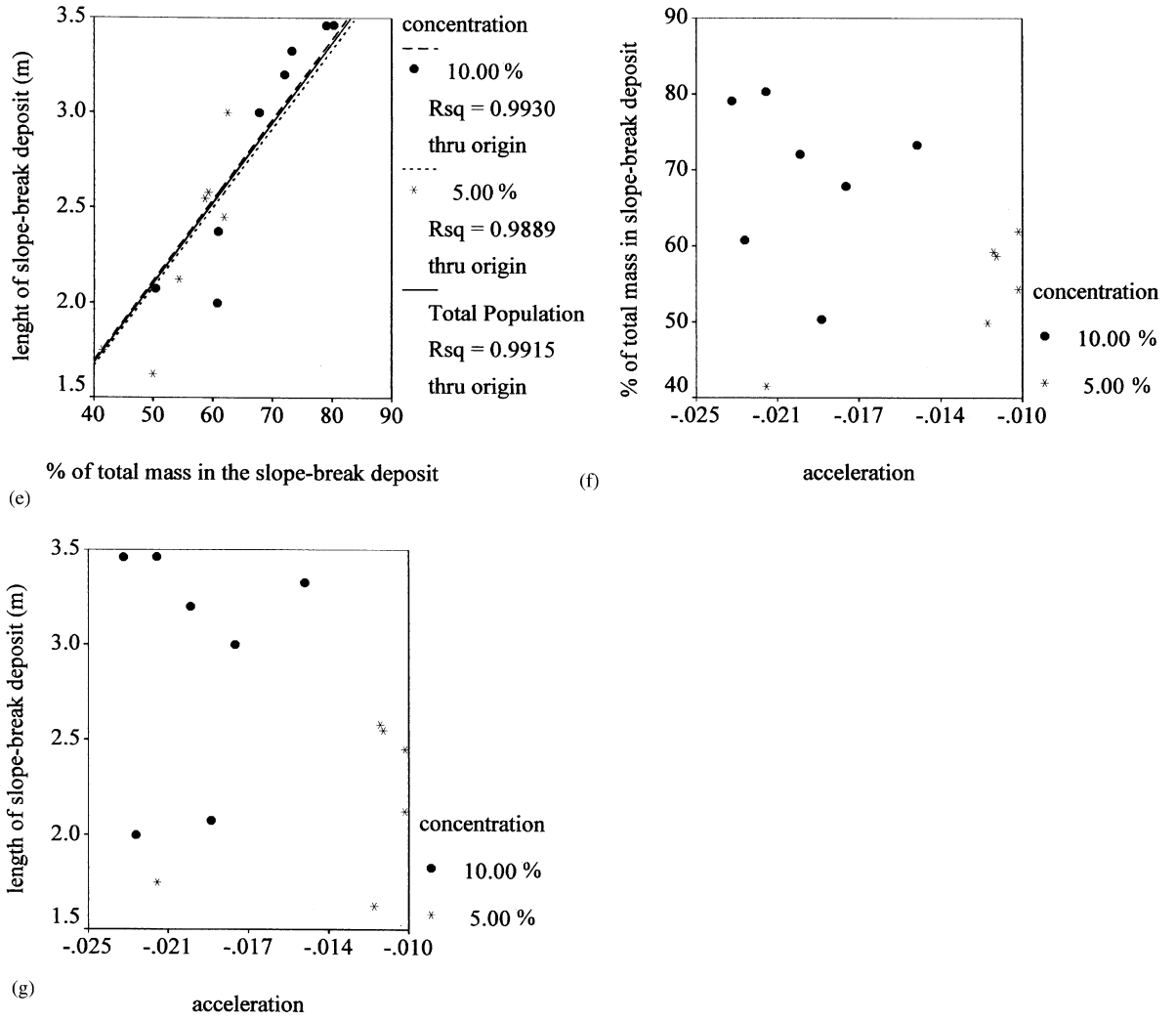

Fig. 4. (*continued*)

5. Discussion: conditions for formation of slope-break deposits

Relationships in Figs. 3 and 4 suggest that the formation of a significant slope-break deposit depends on velocity of a flow near the base of the slope and the angle of slope change. From this it may be inferred that hydraulic jumps may be important for the formation of slope-break deposits. Unfortunately, it is difficult to assess the flow thickness near the slope break because of the generation of increased mixing, consequently we could not easily assess if, or where exactly, a hydraulic jump formed. Definition of the densiometric Froude number is not possible as the suspended sediment concentrations vary continuously during flow and we had no method of measuring it directly. The densiometric Froude number is the parameter which is the most difficult to derive in natural conditions. In addition the vertical variation of concentration can be important, particularly within high-concentration flows (Kneller et al., 1997). Other parameters can be derived in natural conditions:

flow thickness can be estimated using the upper limit of erosion or deposition and flow velocity can be estimated using numerical models and, sometimes, calibrated by cable failures.

Few features in natural deposits have been explained by a strong decrease in slope gradient, potentially producing a hydraulic jump. The Nice slide (Gennesseaux et al., 1980; Malinverno et al., 1988) created a turbidity current that formed a hydraulic jump at the mouth of the Var submarine canyon, 25 km away from the initial slide (Savoye, pers. comm.). In the canyon, the flow was probably very concentrated ($\rho_f = 1350$ kg m^{-3}) and velocities where >25 m s^{-1} (Piper and Savoye, 1993; Mulder et al., 1997). Thickness of the head probably did not exceed 20–30 m (Piper and Savoye, 1993). Beyond the canyon mouth, the current slowed down to less than 10 m s^{-1} and thickened to possibly 150 m (Piper and Savoye, 1993). Downstream of this location, a related turbidite varies in thickness from 0.1 and 1 m (Piper and Savoye, 1993). This extensive turbidite, which covers more than 1500 km^2, can be interpreted as a slope-break deposit formed downstream of the hydraulic jump created in the current at the canyon mouth where a strong slope break occurs (Fig. 5).

Our experiments were all laterally confined flows, but natural hydraulic jumps are also usually associated with a change in flow width, for example when a flow spreads from a channel or a canyon over a fan valley (illustrated by the Nice case study). Such an increase in flow width might increase flow deceleration and enhance the rapid dumping of particles. In such conditions, the downstream extent of the slope-break deposit should be less than predicted by laterally restricted currents as in this paper and the volume of deposits related to the decrease in slope should be larger.

If the velocity of a flow declines suddenly (as occurs at a break of slope) and the sediment flux to the bed increases, it is likely that there may be an increase in the range of sediment sizes being deposited and consequently a decline in sediment sorting. We attempted to test this theory by analysing grain size in samples taken from the deposits. The results suggested that the theory might be correct, but as the sorting of the original sediment is very good the variation in sorting in the deposits was very small and within the error ranges of the method used to assess sorting. The theory however does explain the suggestion of poorer grading in the slope-break deposit than in the rest of the deposits along the runout of the current and may explain some major grain size breaks that are frequently observed in fine turbidites (Piper and Deptuck, 1997). In that case silty-mud lamination in turbidite deposits could be related to the succession of billows created at the slope break and to the related variations in flow velocity and regime in the bottom boundary layer as described in the burst and sweep theory of Hesse and Chough (1980).

Slope-break deposits could also be the explanation for the natural relief that is frequently observed at the base of continental slopes that has been called submarine plunge pools (Farre and Ryan, 1985). These 'plunge pools' have an ovoid shape and occur downslope of breaks in slopes. They are frequently associated with sediment flow deposits or erosional features (Aarseth et al., 1989; Bellaiche, 1993). The relief bordering the plunge pools can be tens of metres high and could result from vertical stacking of slope-break deposits deposited by successive sediment density flows occurring on the continental slope.

6. Conclusions

The laboratory experiments in agreement with earlier work (Dade et al., 1994 and others) suggest that steeper slopes in proximal areas generally result in thinner deposits that extend further. However negative changes in bed slope (abrupt slope break) force change in the characteristics of the density current which in turn controls the distribution of the deposits. The change is not a simple deceleration to that velocity expected on the lower slope but rather it is sufficient to result in an area of excess deposition downstream of the slope break. Such variations, as well as those that can occur when a flow meets an obstacle (Alexander and Morris, 1994), are important in terms of oil reservoirs because thickness of productive sandy layers can vary more than two-fold.

The experimental results suggest that an abrupt change in slope can result in significant variations in turbidite thickness. The deposits related to such a variation are called slope-break deposits.

The length and thickness of the experimental slope-break deposit relate to the velocity of the flow on the

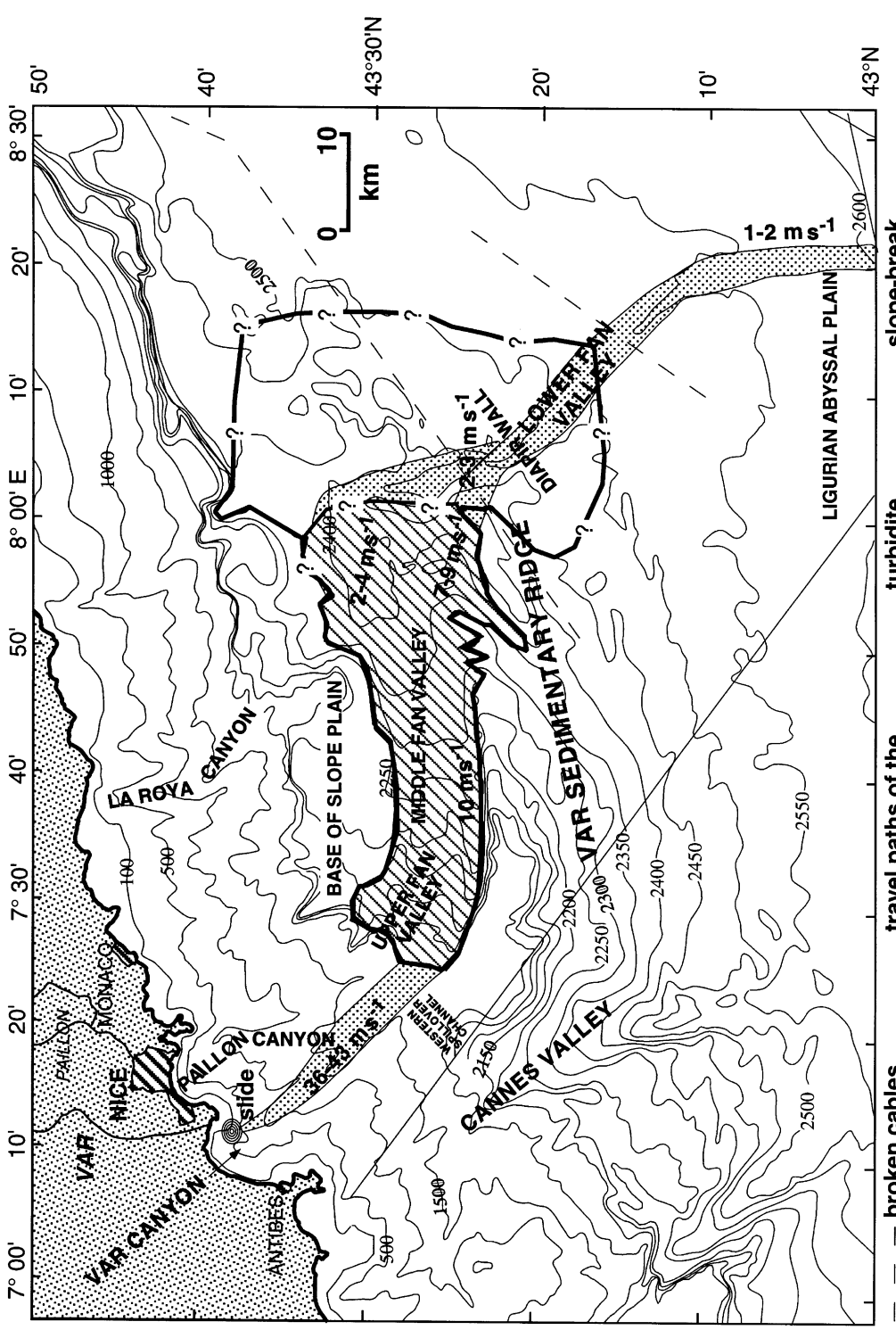

Fig. 5. Pathway of the 1979 slide and turbidity current in the Var Canyon and recognised extension of the related turbidite interpreted in part as a slope-break deposit. Calculated velocities of the flow are indicated (from Piper and Savoye, 1993; Mulder et al., 1997).

slope and the angle of slope change. It is also likely that the slope-break deposit length, and to a lesser extent amplitude, is controlled by particle settling velocities, but this was not assessed in these experiments.

The sediment flux to the bed in the area of a slope-break deposit is controlled by the deceleration of the flow passing over the slope break, and is also influenced by changes in turbulence intensity over the area. The distance over which the effects of the sudden change in slope influences the deposit (i.e. the slope-break deposit length) is additionally dependent on the flow thickness and settling velocity, such that with thick flows with low settling velocity particles the slope-break deposits may be less easy to define.

The volume of the slope-break deposit could be more important if a change in conduit width is associated to the slope decrease. The Var system is a natural example of a slope-break deposit and is associated with channel enlargement.

A future extension of this work could be a combined modelling of slope and channel changes. Simple numerical modelling including conservation of flux could be compared with laboratory experiments. The results could be applied to ancient deposits and allow paleoslope reconstruction where a slope-break deposit is encountered.

Acknowledgements

Thanks to Laurence Badham for help with apparatus construction, Claire Bisault for help with sampling and Julie Herniman for assistance with grain size analysis. This research was undertaken while T. Mulder was a research fellow in Cardiff University funded by the TMR programme of the EU. Authors thank J.-C. Faugères for his useful comments on an early version of the paper, D. Stevens for discussion of the results and B. Dade, J. J. Major and R.L Slingerland for their constructive reviews.

Appendix A

c	suspended solid concentration
c_i	suspended sediment concentration at initiation of experiment
Δh	amplitude of the slope-break deposit
Fr	Froude number
g	acceleration due to gravity
h_b	height of the body of the flow
V	mean flow velocity
V_1	Maximum velocity of the head of the flow on the slope
V_2	Velocity of the head of the flow at the distal end of the slope-break deposit
x	distance along the bed
x_1	distance from the lock gate to the proximal side of the slope-break deposit
x_2	distance from the lock gate to the distal side of the slope-break deposit
x_h	distance from the proximal to the distal side of the slope-break deposit
Z	total mass of sediment in the area of the slope-break deposit (between x_1 and x_2) expressed as a percentage of the total mass of the deposit
α	bed slope
ρ_f	bulk density of the flow
ρ_a	ambient water density

References

Aarseth, I., Lonne, O., Giskeodegaard, O., 1989. Submarine slide in glaciomarine sediments in some western Norwegian fjords. Mar. Geol. 88, 1–21.

Adams, J.r., C, E., Wells, J.T., Park, Y.A., 1990. Internal hydraulics of a sediment-stratified channel flow. Mar. Geol. 95, 131–145.

Adams, E.W., Schlager, W., 2000. Basic types of submarine slope curvature. J. Sed. Res. 70, 814–828.

Alexander, J., Morris, S.A., 1994. Observations on experimental, nonchanelized, high-concentration turbidity currents and variations in deposit around obstacles. J. Sed. Res. A64, 899–909.

Bellaiche, G., 1993. Sedimentary mechanisms and underlying tectonic structures of the northwestern Mediterranean margin, as revealed by comprehensive bathymetric and seismic surveys. Mar. Geol. 112, 89–108.

Carling, P.A., 1995. Flow-separation berms downstream of a hydraulic jump in a bedrock channel. Geomorphology 11, 245–253.

Chanson, H., Montes, J.-S., 1995. Characteristics of undular hydraulic jumps: experimental apparatus and flow patterns. Journal of Hydraulic Engineering, ASCE 121, 129–144.

Cole, P.D., Scarpati, C., 1993. A facies interpretation of the eruption and emplacement mechanisms of the upper part of the Neapolitan Yellow Tuff. Campi Flegrei, southern Italy. Bulletin of Volcanology 55, 311–326.

Collier, R.E.Ll., Leeder, M.R., Trout, M., Ferentinos, G., Lyberis, E., Papatheodorou, G., 2000. High sediment yields and cool wet winters: test of last glacial paleoclimates in the northern Mediterranean. Geology 28, 999–1002.

Dade, W.B., Lister, J.R., Huppert, H.E., 1994. Fine-sediment deposition from gravity surges on uniform slopes. J. Sed. Res. A64, 423–432.

Farre, J.A., Ryan, W.B., 1985. Three-dimensional view of erosional scars on the U.S. Mid-Atlantic continental margin. AAPG Bull. 69, 923–932.

Garcia, M.H., 1993. Hydraulic jumps in sediment-driven bottom currents. Journal of Hydraulic Engineering 119, 1094–1117.

Garcia, M.H., Parker, G., 1989. Experiments on hydraulic jumps in turbidity currents near a canyon-fan transition. Science 245, 393–396.

Gennesseaux, M., Mauffret, A., Pautot, G., 1980. Les glissements sous-marins de la pente continentale niçoise et la rupture de câbles en mer Ligure (Méditerranée occidentale). Académie des Sciences, Paris, Comptes Rendus 290, 959–962.

Gorrell, G., Shaw, J., 1991. Deposition in an esker, bead and fan complex, Lanark, Ontario, Canada. Sedimentary Geology 72, 285–314.

Hesse, R., Chough, S.K., 1980. The Norwest Atlantic Mid-Ocean Channel of the Labrador Sea: II. Deposition of parallel laminated levee-mud from the viscous sublayer of low density currents. Sedimentology 27, 697–711.

Hughes-Clarke, J.E., Shor, A.N., Piper, D.J.W., Mayer, L.A., 1990. Large-scale current-induced erosion and deposition in the path of the 1929 Grand Banks turbidity current. Sedimentology 37, 613–629.

Huppert, H.E., Simpson, J.E., 1980. The slumping of gravity currents. J. Fluid Mechanics 99, 785–799.

Kneller, B.C., Buckee, C., 2000. The structure and fluid mechanics of turbidity currents: a review of some recent studies and their geological implications. Sedimentology 47, 62–94 (Suppl. 1).

Kneller, B.C., McCaffrey, W.D., Bennet, S.J., 1997. Velocity and turbulence structure of density currents and internal solitary waves: potential sediment transport and the formation of waves ripples in deep water. Sedimentary Geol. 112, 235–250.

Komar, P.D., 1971. Hydraulic jumps in turbidity currents. Geol. Soc. Am. Bull. 82, 1477–1488.

Komar, P.D., 1973. Continuity of turbidity current flow and systematic variations in deep-sea channel morphology. Geol. Soc. Am. Bull. 84, 3329–3338.

Komar, P.D., 1975. Supercritical flow in density currents: a discussion. J. Sed. Petrol. 45, 747–749.

Laval, A., Cremer, M., Beghin, P., Ravenne, C., 1988. Density surges: two-dimensional experiments. Sedimentology 35, 73–84.

Malinverno, A., Ryan, W.B.F., Auffret, G.A., Pautot, G., 1988. Sonar images of recent failure events on the continental margin off Nice, France. Geol. Soc. Am. Special Paper 229, 59–75.

Masson, D.G., 1994. Late Quaternary turbidity current pathways to the Madeira Abyssal Plain and some constraints on turbidity current mechanisms. Basin Res. 6, 17–33.

Menard, H.W., 1964. Marine Geology of the Pacific. McGraw-Hill, New York, p. 271.

Middleton, G.V., 1966a. Small scale models of turbidity currents and the criterion for auto-suspension. J. Sed. Petrol. 36, 202–208.

Middleton, G.V., 1966b. Experiments on density and turbidity currents. I. Motion of the head. Can. J. Earth Sci. 3, 523–546.

Middleton, G.V., 1966c. Experiments on density and turbidity currents. II. Uniform flow of density currents. Can. J. Earth Sci. 3, 627–637.

Middleton, G.V., 1967. Experiments on density and turbidity currents. III. Deposition of sediment. Can. J. Earth Sci. 4, 475–505.

Middleton, G.V., 1993. Sediment deposition from turbidity currents. Annual Review of Earth Planetary Sci. 21, 89–114.

Middleton, G.V., Hampton, M.A., 1973. Sediment gravity flows: mechanics of flow and deposition. In: Middleton, G.V., Bouma, A.H. (Eds.), Turbidity and Deep Water Sedimentation, S.E.P.M. Pacific Section, Short Course Lecture Notes, SEPM, Los Angeles, pp. 1–38.

Mulder, T., Alexander, J., 2001. The physical character of subaqueous sedimentary density currents and their deposits. Sedimentology 48 in press.

Mulder, T., Savoye, B., Syvitski, J.P.M., 1997. Numerical modelling of a mid-sized gravity flow: the 1979 Nice turbidity current (dynamics, processes, sediment budget and seafloor impact). Sedimentology 44, 305–326.

Nardin, T.R., Hein, F.J., Gorsline, D.S., Edwards, B.D., 1979. A review of mass movement processes, sediment and acoustic characteristics, and contrasts in slope and base-of-slope systems versus canyon-fan-basin floor systems. In: Doyle, L.J., Pilkey, O.H. (Eds.), Geology of Continental Slopes S.E.P.M., Spec. Publ., 27, 61–73.

Papatheodorou, G., Ferentinos, G., 1993. Sedimentation processes and basin-filling depositional architecture in an active asymmetric graben: Strava graben: Gulf of Corinth, Greece. Basin Res. 5, 235–253.

Piper, D.J.W., Deptuck, M., 1997. Fine-grained turbidites of the Amazon fan: facies characterisation and interpretation. In: Flood, R.D., Piper, D.J.W., Klaus, A., Peterson, L.C. (Eds.), Proceedings of the Ocean Drilling Program, Scientific Results, 155, 79–108.

Piper, D.J.W., Savoye, B., 1993. Processes of late Quaternary turbidity current flow and deposition on the Var deep-sea fan, north-west Mediterranean Sea. Sedimentology 40, 557–582.

Ravenne, C., Beghin, P., 1983. Apport des expériences en canal à l'interprétation sédimentologique des dépôts de cônes détritiques sous-marins. Revue de l'Institut Français du Pétrole 38, 279–297.

Rimoldi, B., Alexander, J., Morris, S., 1996. Experimental turbidity currents entering density-stratified water: analogues for turbidites in Mediterranean hypersaline basins. Sedimentology 43, 527–540.

Rooksby, S.K., 1991. The miller field, blocks 16/7b, 16/7a, UK North Sea. In: Abbotts, I.L. (Ed.), United Kingdom Oil and Gas Fields 25 Years Commemorative Volume. Mem. Geology Society, London 14, 159–164.

Sarkar, S., Bose, P.K., Bandhyopadhayay, S., 1991. Intertidal occurrence of mesoscale scours in the Bay of Bengal, India, and their implications. Sed. Geol. 75, 29–37.

Syvitski, J.P.M., Schafer, C.T., 1996. Evidence for an earthquake-triggered basin collapse in Saguenay Fjord, Canada. Sed. Geol. 104, 127–153.

Weirich, F.H., 1988. Field evidence for hydraulic jumps in subaqueous sediment gravity flows. Nature 332, 626–629.

Weirich, F.H., 1989. The generation of turbidity currents by subaerial debris flows, California. Geol. Soc. Am. Bull. 101, 278–291.